J. Fluid Mech. (1965), *vol.* 23, *part* 1, *pp.* 145–172
Printed in Great Britain

Some effects of stratification and geometry in rotating fluids

By G. F. CARRIER
Harvard University

(Received 12 January 1965 and in revised form 8 April 1965)

The phenomena which occur in a fluid contained in a rotating system are strongly influenced by the density gradients in that fluid and by certain features of the geometry. In this paper, we study several specific phenomena which involve stratification and/or irregular surface topography and some phenomena which arise because of an equatorial geometry. Although several of these studies are motivated by particular geophysical questions, we do not treat comprehensively any geophysical phenomenon. Nevertheless, the inferences we draw from these studies do much to clarify the roles of the mechanisms underlying various geophysical phenomena and these inferences should be of value when comprehensive geophysical investigations are attempted.

1. Introduction

When density gradients are present in the fluid in a system which rotates at speed $\boldsymbol{\Omega}$, the phenomena which occur can differ markedly from those described in Carrier (1965).† The analyses needed to predict such phenomena are direct extensions of those appropriate to the non-stratified fluid and the flows can be characterized with analogous simplicity. Further modifications are implied when the geometry is not axially symmetric and, in particular, the flow of a stratified fluid in a region with irregularities in bottom topography is of great interest.

Modifications of the phenomena and of the associated analytical techniques also arise when the geometry of the configuration studied is such that, somewhere on the boundary surface described by $F(x,y,z) = 0$, $\boldsymbol{\Omega}.\mathrm{grad}\,F$ changes continuously from positive to negative values. We call this an equatorial geometry because the geophysical phenomena in the equatorial regions of our planet provide the strongest motivation for the study of such configurations.

Specifically, this paper contains the following studies:

(1) A highly simplified theory for the axially symmetric flow of a rotating fluid of uniform density.

(2) A theory for axially symmetric flow in a system containing two or more layers of fluid, each of constant density.

(3) A study of axially symmetric flow of a fluid of varying density which takes account in a crude way of any diffusive mechanisms which may be present (e.g. small-scale natural convection, turbulent diffusion, etc.). The principal objective (and result) is the identification of the parameter which determines whether the

† Henceforth referred to, for brevity, as [1].

fluid acts like a fluid with constant density, a multi-layered fluid, or neither of the foregoing.

(4) A general theory of three-dimensional flow in a configuration whose top surface is perpendicular to the rotation axis and whose depth contour has slopes which are large compared to $(\nu/\Omega L^2)^{\frac{1}{2}}$.† The modification required to account for topography at the top would be extremely simple.

(5) An examination of a particular flow configuration of the foregoing type. The region is an annulus whose bottom contour is shown in figure 8 and defined by equation (3.20). The motion is driven by moving the top surface in the circumferential θ-direction at a speed given by equation (3.21) and shown in figure 9. If the bottom were flat, the velocity in most of the fluid would be independent of the axial co-ordinate, it would have zero radial and axial components, and its magnitude (as a function of the radial co-ordinate η), would be half that of figure 9. With the bottom topography of figure 8, the flow is cellular and very slow compared to the imposed surface velocity; the fluid over each segment of constant slope never leaves that region and the velocity shown in figure 11 is that which would prevail everywhere except near the junctions of adjacent segments. A plan view of the velocity field including the 'turn around' regions near these junctions is shown in figure 10.

(6) The flow in a second geometry. This time the bottom topography is given by figure 12 and the imposed top surface motion is again given by figure 9. The motion over ABC of figure 12 is the same as in the previous problem except for *details* near the 'turn around' regions. The flow in the flat region is one half that of figure 9 plus a uniform flow of opposite sign. That is, the flow over the flat bottom is that of figure 14. The plan view of this velocity field is shown in figure 13.

These flows indicate very clearly the enormous constraint implied by the presence of both rotation and variable depth.

(7) The flow in a two-layer system in which the top layer is of uniform depth and the lower layer has bottom topography. The flow in one layer differs enormously from that in the other, and topography alone *could* account for the fact that the flows on opposite sides of the oceanic thermocline are so different.

(8) A general formalism for the study of flows in equatorial regions and its application to the flow in a thin equatorial layer. The variety of flow patterns which emerges for a small family of geometries (layer thickness varying as a function of latitude) implies that the possibilities of linear models have not been exhausted by previous linear studies. It is the author's opinion, based on the results of § 4, that no single-layer theory will provide a satisfactory understanding of the Cromwell current but that an appropriate *linear* theory may account for much of the phenomenon.

2. Stratified fluids

When a fluid of uniform density in the axially symmetric rotating system of figure 1 is required to move at the surface AB with a peripheral speed

$$v(r, L) = r\Omega f(r)$$

† ν is the kinematic viscosity (molecular or eddy as appropriate), Ω the angular velocity of the system, L a characteristic length.

relative to the rigidly rotating reference state, the motion is characterized by:

(1) Frictional boundary layers (Ekman layers) of thickness $(\nu/\Omega)^{\frac{1}{2}}$ along AB and A'B'.

(2) Regions I, II and III in which the relative peripheral velocity is $v(r, z) = 0$, $v(r, z) = \Omega r f(r)/2$, $v(r, z) = 0$, respectively.

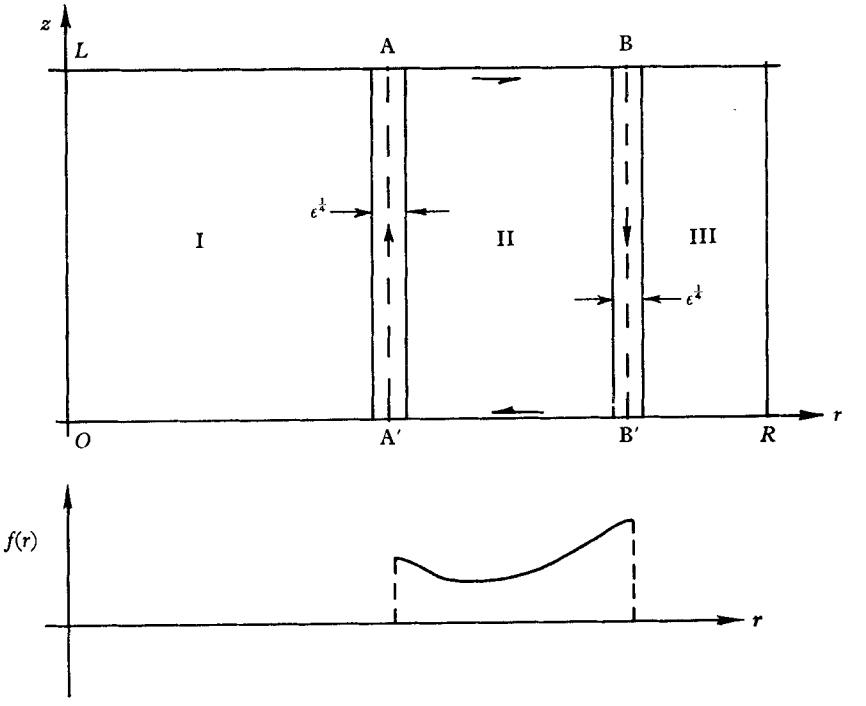

FIGURE 1. Flow configuration discussed in the introductory remarks. $\Omega r f(r)$ is the peripheral velocity imposed at $z = L$. The arrows on the broken lines denote the location and direction of the internal currents which are present when $f(r)$ is positive.

(3) Annular regions of width $(\nu/\Omega)^{\frac{1}{4}} L^{\frac{1}{2}}$ along AA' and BB' in which the diffusion of angular momentum and vorticity is countered by the radial convection of angular momentum and by axial vortex line stretching. In particular, fluid emerges at B from the upper Ekman layer in the amount

$$\int_{z_0}^{L} u\, dz = \left(\frac{\nu}{2\Omega}\right)^{\frac{1}{2}} \frac{f(B)}{2} B\Omega,$$

(where u is radial velocity component) and is transported along the diffusive layer about BB' to the lower Ekman layer.

The foregoing statements are accurate whenever

$$\nu/\Omega L^2 \ll 1, \quad \nu L^2/\Omega \ll R^4, \quad |f'(r)/f_{\max}| \ll (\nu/\Omega)^{-\frac{1}{4}} L^{-\frac{1}{2}} \quad \text{and} \quad |f(r)| \ll 1.$$

That this kind of characterization is valid for much more complicated configurations is illustrated in [1] but, for the forthcoming material, the presentation gains greatly in simplicity when we confine our attention, initially, to the simple geometry of figure 1.

Suppose now that the container is filled with two immiscible incompressible fluids as in figure 2 and that there is a uniform gravitational field in the negative z-direction. Suppose, furthermore, that the difference in density of the two fluids, the gravitational acceleration g, the angular speed Ω, and the size of the container are such that, in the uniformly rotating state, the interface slope $h'(r)$ is at most

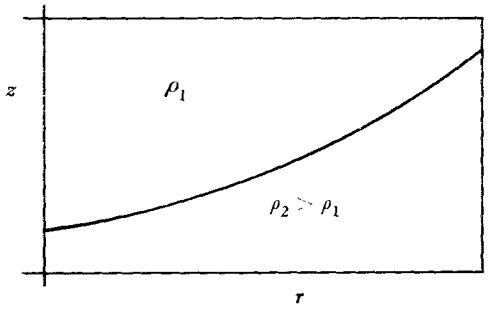

FIGURE 2. Ambient (rigidly rotating) configuration for stratified fluid.

of order unity. Under these circumstances, the flow pattern induced by the surface motion, $f(r)$, cannot resemble that described above for the single fluid of constant density. In fact, the interface can be distorted only by an amount consistent with the pressure discrepancy induced by the imposed surface motion and, since $f(r) \ll 1$, the change in interface-slope so implied will be small compared to the ambient interface-slope. Accordingly, we must seek a steady-flow pattern in which the usual frictional boundary conditions at the container surface are met, in which no fluid crosses the interface, and in which velocity and stress are continuous across the interface.

First, however, we must develop a greatly simplified framework within which many configurations can be studied.

2.1. *Simplified theory for one-layer axi-symmetric flows*

We have already seen in [1] that, except in narrow cylindrical layers about AA′ and BB′, the flow in the configuration of figure 1 can be described by†

$$v(\eta,x) = V(\eta)+A(\eta)\exp\{(i/\epsilon)^{\frac{1}{2}}(x-1)\}+B(\eta)\exp\{(-i/\epsilon)^{\frac{1}{2}}(x-1)\} + C(\eta)\exp\{-(i/\epsilon)^{\frac{1}{2}}x\}+D(\eta)\exp\{-(-i/\epsilon)^{\frac{1}{2}}x\},$$

and

$$\psi(\eta,x) = \Psi(\eta)+A_1(\eta)\exp\{(i/\epsilon)^{\frac{1}{2}}(x-1)\}+B_1(\eta)\exp\{(-i/\epsilon)^{\frac{1}{2}}(x-1)\} + C_1(\eta)\exp\{-(i/\epsilon)^{\frac{1}{2}}x\}+D_1(\eta)\exp\{-(-i/\epsilon)^{\frac{1}{2}}x\},$$

where $x = z/L$, $\eta = r/L$, $\epsilon = \nu/2\Omega L^2$, $\mathbf{v}(r,z) = \Omega R[\hat{\boldsymbol{\theta}}v(\eta,x) - \operatorname{curl}\hat{\boldsymbol{\theta}}\psi(\eta,x)]$, and where we have confined our investigations to those for which v and ψ are small enough that all non-linear contributions to the momentum balance can be ignored.

† Throughout this paper there is a distressing but unavoidable multiplicity of notation. Whenever possible, lower case letters ($u, v, w, p, \psi, \ldots$) denote complete descriptions of the field variables (velocity, pressure, potential, etc.); capital letters ($U, V, \ldots$) denote field descriptions away from the boundary layers. Numerical subscripts (except zero) identify the region to which the variable refers but V_0, for example, is an interface velocity. Finally, $V_+, U_+, \ldots$ denote velocity components at a top surface and the subscript '$-$' refers to a bottom surface.

Guided by this experience, we expect the flow in the more general axially symmetric configuration of figure 3 to be characterized by similar boundary layers and we adopt the descriptions,

$$v(\eta, x) = V(\eta) + F_1(\eta, [x - d(\eta)]/\sqrt{\epsilon}) + F_2(\eta, [x - b(\eta)]/\sqrt{\epsilon}), \tag{2.1}$$

$$\psi(\eta, x) = \Psi(\eta) + G_1(\eta, [x - d(\eta)]/\sqrt{\epsilon}) + G_2(\eta, [x - b(\eta)]/\sqrt{\epsilon}), \tag{2.2}$$

except in cylindrical layers of width $\Delta\eta$, whose order of magnitude is not greater than $\epsilon^{\frac{1}{4}}$; these layers (in which radial diffusion will play an important role) will

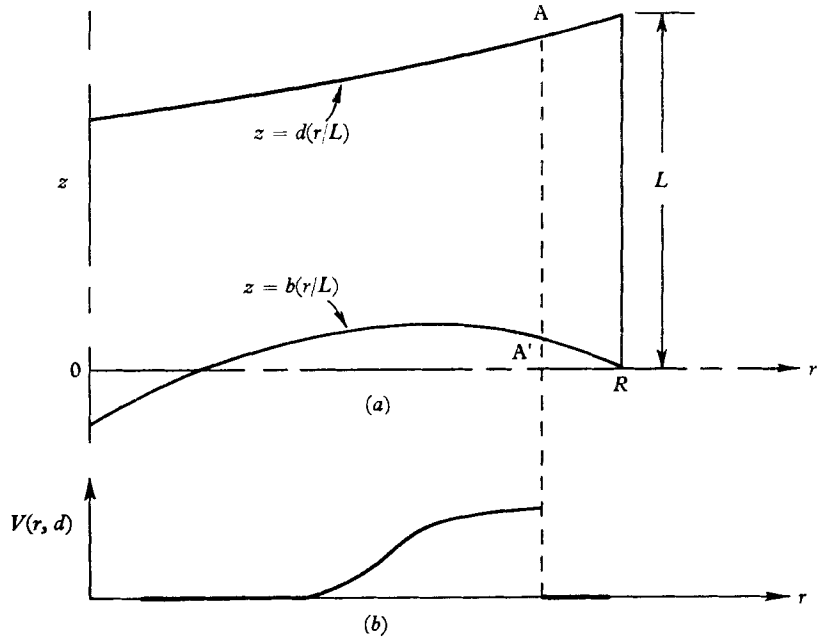

FIGURE 3. Configuration of § 2.1. (*a*) Interface profiles. (*b*) Surface velocity distribution.

be located wherever the boundary conditions imply an abrupt change in behaviour. For the $v(\eta, d(\eta))$ depicted in figure 3, for example, such a layer will lie along AA'.

In the absence of contributions from the (non-linear) $\mathbf{v}.\mathrm{grad}\,\mathbf{v}$ terms, the conservation of mass and momentum imply [1] that

$$\epsilon\Delta\Delta\psi + v_x = 0, \tag{2.3}$$

$$\epsilon\Delta v - \psi_x = 0. \tag{2.4}$$

Within the usual framework of boundary-layer theory, equations (2.3) and (2.4) impose no constraints on the choice of $V(\eta)$ and $\Psi(\eta)$ when equations (2.1) and (2.2) are substituted into them; they do require, however, that, to order $\sqrt{\epsilon}$,

$$\epsilon\lambda^4 G_{1,xxxx} + F_{1,x} = 0, \quad \epsilon\lambda^2 F_{1,xx} - G_{1,x} = 0,$$

and

$$\epsilon\sigma^4 G_{2,xxxx} + F_{2,x} = 0, \quad \epsilon\sigma^2 F_{2,xx} + G_{2,x} = 0,$$

where $\lambda^2 = 1 + [d'(\eta)]^2$, $\sigma^2 = 1 + [b'(\eta)]^2$.

We seek a solution of these under boundary conditions which require that

$$\psi[\eta, d(\eta)] = \psi[\eta, b(\eta)] = 0,$$
$$\psi_x[\eta, d] = U_+(\eta), \quad \psi_x[\eta, b] = U_-(\eta),$$
$$v[\eta, d] = V_+(\eta), \quad v[\eta, b] = V_-(\eta).$$

The solutions F_i and G_i are clearly of exponential type and the application of the foregoing boundary conditions implies that

$$V(\eta) = [\lambda^{\frac{1}{2}}V_+(\eta) + \sigma^{\frac{1}{2}}V_-(\eta) + \lambda^{\frac{3}{2}}U_+(\eta) + \sigma^{\frac{3}{2}}U_-(\eta)]/[\lambda^{\frac{1}{2}} + \sigma^{\frac{1}{2}}], \tag{2.5}$$
$$\Psi(\eta) = -(\tfrac{1}{2}\epsilon)^{\frac{1}{2}}[V_+(\eta) - V_-(\eta) + \lambda U_+(\eta) - \sigma U_-(\eta)]/[\lambda^{-\frac{1}{2}} + \sigma^{-\frac{1}{2}}]. \tag{2.6}$$

The dimensionless surface tractions are

$$v_x(\eta, d) = -\Psi(\eta)/\epsilon\lambda^2, \tag{2.7}$$
$$v_x(\eta, b) = -\Psi(\eta)/\epsilon\sigma^2; \tag{2.8}$$
$$\Psi_{xx}(\eta, d) = (2/\epsilon\lambda^3)^{\frac{1}{2}}U_+ + \Psi/\epsilon\lambda^3, \tag{2.9}$$
$$\psi_{xx}(\eta, b) = -(2/\epsilon\sigma^3)^{\frac{1}{2}}U_- + \Psi/\epsilon\sigma^3. \tag{2.10}$$

Thus we see that the flow has the same general character as that of figure 1 but that the actual recipes depend on the details of $b(\eta)$ and $d(\eta)$. We also note in passing that the diffuse cylindrical layer along AA′ of figure 3 could be calculated by the methods used in [1] and appended to the above description.

For those situations in which the effective viscosity associated with the lateral transmission of stress is different from that for vertical stress transmission, one can use an appropriate value of ν in appending these friction layers without regard to the value which was used in the Ekman layer analysis. This remark applies throughout the paper but no further discussion of it will appear since the numerical choice for ν will not affect the *character* of the flows we study.

2.2. *Multi-layer axially symmetric flows*

Consider now the two-layer rotating system which has the geometry of figure 2 when in a state of rigid rotation but let the fluid at the top and at the bottom be given the relative motion

$$v(\eta, 1) = V_+(\eta),$$
$$u(\eta, 1) = v(\eta, 0) = u(\eta, 0) = 0.$$

We describe the motion at the interface by $v(\eta, b(\eta)) = V_0$ and $\psi_x(\eta, b(\eta)) = U_0$, and we denote by subscripts 1 and 2 the properties of the upper and the lower fluids, respectively.

Using the results of the foregoing section, we have, for the upper layer,

$$V_1(\eta) = [V_+(\eta) + \sigma^{\frac{1}{2}}V_0 + \sigma^{\frac{3}{2}}U_0]/(1 + \sigma^{\frac{1}{2}}), \tag{2.11}$$
$$\Psi_1(\eta) = (\tfrac{1}{2}\epsilon_1)^{\frac{1}{2}}(V_0 - V_+ + \sigma U_0)/(1 + \sigma^{-\frac{1}{2}}), \tag{2.12}$$

and, for the lower layer,

$$V_2(\eta) = (\sigma^{\frac{1}{2}}V_0 + \sigma^{\frac{3}{2}}U_0)/(1 + \sigma^{\frac{1}{2}}), \tag{2.13}$$
$$\Psi_2(\eta) = -(\tfrac{1}{2}\epsilon_2)^{\frac{1}{2}}(V_0 + \sigma U_0)/(1 + \sigma^{-\frac{1}{2}}). \tag{2.14}$$

We also require that the surface tractions μv_x and $\mu\psi_{xx}$ be continuous at $x = b(\eta)$. Thus, according to equations (2.7) through (2.10),

$$\mu_1 \Psi_1/\epsilon_1 = \mu_2 \Psi_2/\epsilon_2 \tag{2.15}$$

and

$$U_0 = 0. \tag{2.16}$$

Equations (2.11) through (2.16) imply that, with $k = (\rho_2\mu_2/\rho_1\mu_1)^{\frac{1}{2}}$,

$$V_0 = V_+/(1+k), \tag{2.17}$$

$$V_1 = [(1+k+\sigma^{\frac{1}{2}})/(1+\sigma^{\frac{1}{2}})(1+k)]V_+, \tag{2.18}$$

$$V_2 = \sigma^{\frac{1}{2}}V_+/(1+k)(1+\sigma^{\frac{1}{2}}), \tag{2.19}$$

$$\Psi_1 = (\rho_2/\rho_1)\Psi_2 = -(\tfrac{1}{2}\epsilon_1)^{\frac{1}{2}}kV_+/(1+k)(1+\sigma^{-\frac{1}{2}}). \tag{2.20}$$

We could now use the foregoing velocity distributions and the original momentum equations to determine the pressure distribution in each fluid. We could then find

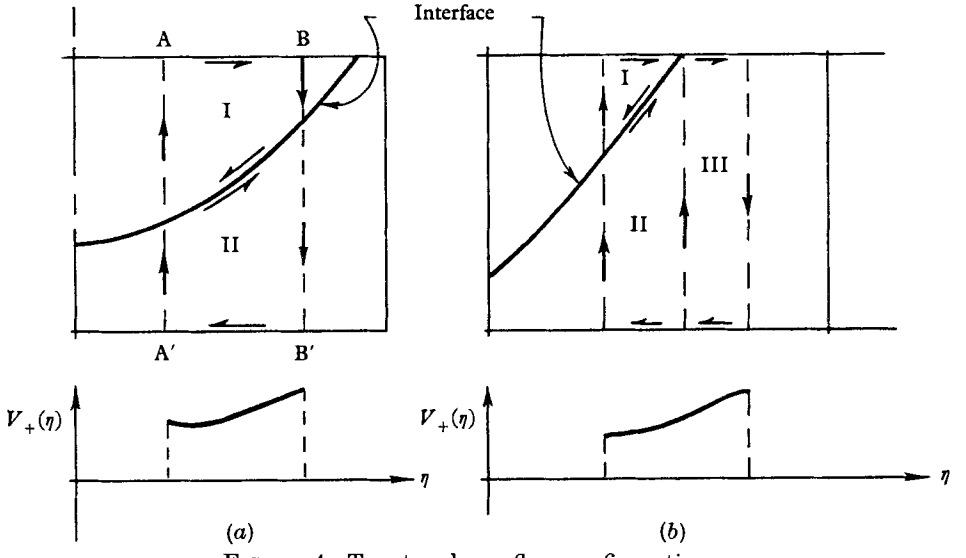

FIGURE 4. Two two-layer flow configurations.

In (*a*),

$$V_{\rm I} \simeq \tfrac{3}{4}V_+(\eta), \quad V_{\rm II} \simeq \tfrac{1}{4}V_+(\eta).$$

In (*b*), (for $k = 1$)

$$V_{\rm I} \simeq \frac{2+\sigma^{\frac{1}{2}}}{2(1+\sigma^{\frac{1}{2}})}V_+, \quad V_{\rm II} \simeq \frac{\sigma^{\frac{1}{2}}}{2(1+\sigma^{\frac{1}{2}})}V_+, \quad V_{\rm III} = \tfrac{1}{2}V_+.$$

The arrows indicate the intense currents associated with the chosen $V_+(\eta)$.

that surface on which the two pressures were equal and this would be the perturbed position of the interface. We omit the calculation because, in any situation to which the linear and axially symmetric analysis is appropriate, the perturbation in interface position cannot affect the character of the flow nor can it even alter the numbers appreciably.

Figure 4 depicts two illustrative configurations which may provide a simple view of the implications of the foregoing.

Although the inclusion of details is not really justified, it seems worth-while to append a characterization of the flow which occurs in the multi-layer system of

figure 5. No understanding is lost and many fewer symbols are needed when we restrict the results to situations in which $\mu_1 \simeq \mu_2 \simeq \mu_3 \ldots$, $\rho_1 \simeq \rho_2 \simeq \rho_3 \ldots$ and for which the gravitational field is so strong that the interfaces are nearly horizontal. For such flows

$$V_n(\eta) = (2n-1)V_+(\eta)/2N \quad (1 \leqslant n \leqslant N), \tag{2.21}$$

and the interface speeds Y_n are

$$Y_n(\eta) = nV_+(\eta)/N \quad (0 \leqslant n \leqslant N). \tag{2.22}$$

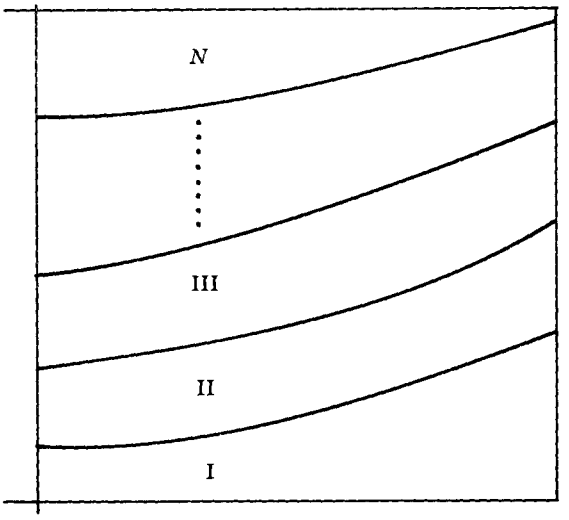

FIGURE 5. Multi-layered flow configuration to which equations (2.21) and (2.22) apply.

One might try to anticipate the behaviour of a fluid having a continuous density variation by adopting an approximation in which there are N distinct layers, each having constant density. When such an approximation is followed by a limit process in which $N \to \infty$ in equation (2.21), the velocity so obtained has the property that $\mathbf{v}.\mathrm{grad}\,\rho = 0$. Clearly, since such a limit process ignores the motion in the Ekman layers, it cannot be accepted at face value. However, we shall see in the next section that such an extrapolation can be valid under rather special conditions.

2.3. *Flows with a continuous density gradient*

We study here the flow which ensues in the configuration of figure 1 when the fluid is 'incompressible' but of varying density. We use quotation marks on 'incompressible' because we will take account of any transport processes which can modify the density of a given parcel of fluid. Such density modifications might be accomplished in the ocean, for example, by the diffusive-convective transfer of salt and heat. We model any such processes by an equivalent diffusion. To be precise, in fact, we write

$$k\Delta\rho = \mathbf{v}.\mathrm{grad}\,\rho. \tag{2.23}$$

where $\mathbf{v}$ is the velocity field (measured relative to the rotating system), ρ is the density field and k is a composite diffusion coefficient which is taken to model all density modifying processes whose scales are small compared to that of $\mathbf{v}$.

In order to get explicit and simply interpreted results, we confine our attention to configurations for which the gravitational field is so strong that the surfaces of constant density (in the ambient rigidly rotating state) are almost horizontal. We also require that $\hat{\mathbf{z}}.\operatorname{grad}\rho_0(r,z)$ be well approximated by $\beta\rho_a/L$, where ρ_0 is the ambient density distribution, ρ_a is the average density, and β a small constant. We prescribe as boundary conditions on ρ

$$\rho(r,L)=\rho_0(r,L), \quad \rho(r,-L)=\rho_0(r,-L). \tag{2.24}$$

Note that, in this section, $2L$ is the depth of the container.

The linearized equations implying the conservation of mass and momentum in this system are

$$\operatorname{div}\mathbf{v}=0, \tag{2.25}$$

$$k\,\Delta\rho'=\mathbf{v}.\operatorname{grad}\rho_0 \tag{2.26}$$

and

$$2\rho_a\,\boldsymbol{\Omega}\times\mathbf{v}+\operatorname{grad}p'+\rho' g\hat{\mathbf{z}}-\hat{\mathbf{r}}\rho'\Omega^2 r=\mu\,\Delta\mathbf{v}, \tag{2.27}$$

where $\rho'=\rho-\rho_0$ and p' is the pressure perturbation, $p-p_0$. In the rigidly rotating state,

$$\operatorname{grad}p_0+\rho_0 g\hat{\mathbf{z}}-\rho_0\Omega^2 r\hat{\mathbf{r}}=0, \tag{2.28}$$

and the curl of (2.28) gives

$$\rho_{0,r}=-\Omega^2 r\rho_{0,z}/g.$$

Since $\rho_{0,z}\simeq-\beta$, equation (2.26) becomes

$$k\,\Delta\rho'=\rho_0(\Omega^2 r/g)\,\beta u-\rho_0\beta w, \tag{2.29}$$

where u and w are the radial and axial components of $\mathbf{v}$.

We define,

$$q=R\rho'/L\rho_a, \quad \epsilon=\mu/2\rho_a\,\Omega L^2 \quad \text{and} \quad \mathbf{v}=R\Omega[\hat{\boldsymbol{\theta}}v(\eta,x)-\operatorname{curl}\hat{\boldsymbol{\theta}}\psi(\eta,x)],$$

where $\eta=r/L$, $x=z/L$; with these definitions, the θ-component of equation (2.27), the θ-component of its curl and equation (2.29) become

$$\epsilon\Delta v-\psi_x=0, \tag{2.30}$$

$$\epsilon\Delta\Delta\psi+(v_x-\beta v)+(g/2\Omega^2 L)\,q_\eta+\tfrac{1}{2}\eta q_x=0 \tag{2.31}$$

and

$$(k/2\Omega L^2)\,\Delta q-\tfrac{1}{2}\beta\psi_\eta-(\Omega^2 L\beta/2g)\,\eta\psi_x=0. \tag{2.32}$$

We anticipate the now familiar boundary-layer structure† and we describe v,ψ,q by

$$v=V(\eta,x)+v_1(\eta,\epsilon^{-\frac{1}{2}}\{x-1\})+v_2(\eta,\epsilon^{-\frac{1}{2}}\{x+1\}), \tag{2.33}$$

$$\psi=\Psi(\eta,x)+\psi_1(\eta,\epsilon^{-\frac{1}{2}}\{x-1\})+\psi_2(\eta,\epsilon^{-\frac{1}{2}}\{x+1\}), \tag{2.34}$$

$$q=Q(\eta,x)+q_1(\eta,\epsilon^{-\frac{1}{2}}\{x-1\})+q_2(\eta,\epsilon^{-\frac{1}{2}}\{x+1\}). \tag{2.35}$$

† But we have no basis on which to anticipate that, as in § 2.1, V, Ψ, Q are functions of η only!

When these descriptions are substituted into (2.30) to (2.32) and the usual boundary-layer arguments are invoked, we see that, for $i = 1, 2$,

$$\epsilon v_{i,xx} - \psi_{i,x} = 0, \tag{2.36}$$

$$\epsilon\psi_{i,xxxx} + v_{i,x} + \tfrac{1}{2}\eta q_{i,x} = 0, \tag{2.37}$$

and

$$(k/2\Omega L^2)\, q_{i,xx} - (\Omega^2 L/2g)\,\beta\eta\psi_{i,x} = 0. \tag{2.38}$$

We also obtain

$$\Psi_x = 0, \tag{2.39}$$

$$V_x + (g/2\Omega^2 L)\, Q_\eta + \tfrac{1}{2}\eta Q_x = 0, \tag{2.40}$$

and

$$(k/2\Omega L^2)\,\Delta Q - \tfrac{1}{2}\beta\Psi_\eta = 0. \tag{2.41}$$

The highly differentiated terms of equation (2.41) must be retained because, for many interesting values $\rho\beta$ and k, it contributes to the mass balance in an important way.

The solutions of (2.36) to (2.38) are

$$v_1 = A\exp\{a(i/\epsilon)^{\frac{1}{2}}(x-1)\} + B\exp\{a(-i/\epsilon)^{\frac{1}{2}}(x-1)\},$$
$$\psi_1 = a(i\epsilon)^{\frac{1}{2}} A\exp\{a(i/\epsilon)^{\frac{1}{2}}(x-1)\} + a(-i\epsilon)^{\frac{1}{2}} B\exp\{a(-i/\epsilon)^{\frac{1}{2}}(x-1)\},$$
$$q_1 = (\Omega^2 L\nu/2gk)\,\beta\eta v_1,$$

where

$$a = (1 + \nu\Omega^2 L\beta\eta^2/k4g)^{\frac{1}{4}}.$$

When $a - 1 \ll 1$, the arithmetic is simplified considerably and, since this inequality is consistent with many geophysical situations and with the constraints we have already imposed on ρ_0, we adopt it. Thus, replacing a by unity, we have

$$v_1 \simeq A\exp\{(i/\epsilon)^{\frac{1}{2}}(x-1)\} + B\exp\{(-i/\epsilon)^{\frac{1}{2}}(x-1)\}, \tag{2.42}$$

$$\psi_1 \simeq (i\epsilon)^{\frac{1}{2}} A\exp\{(i/\epsilon)^{\frac{1}{2}}(x-1)\} + (-i\epsilon)^{\frac{1}{2}} B\exp\{(-i/\epsilon)^{\frac{1}{2}}(x-1)\}, \tag{2.43}$$

$$q_1 \simeq 0, \tag{2.44}$$

$$v_2 \simeq C\exp\{-(i/\epsilon)^{\frac{1}{2}}(x+1)\} + D\exp\{-(-i/\epsilon)^{\frac{1}{2}}(x+1)\}, \tag{2.45}$$

$$\psi_2 \simeq -(i\epsilon)^{\frac{1}{2}} C\exp\{-(i/\epsilon)^{\frac{1}{2}}(x+1)\} - (-i\epsilon)^{\frac{1}{2}} D\exp\{-(-i/\epsilon)^{\frac{1}{2}}(x+1)\}, \tag{2.46}$$

$$q_2 \simeq 0. \tag{2.47}$$

These, together with the boundary conditions

$$\psi(\eta, 1) = \psi(\eta, -1) = \psi_x(\eta, 1) = \psi_x(\eta, -1) = v(\eta, -1) = 0, \tag{2.48}$$

$$v(\eta, 1) = V_+(\eta), \tag{2.49}$$

and equations (2.33) to (2.35), imply

$$V(\eta, 1) - 2^{\frac{1}{2}}\epsilon^{-\frac{1}{2}}\Psi(\eta, 1) = V_+(\eta), \tag{2.50}$$

$$V(\eta, -1) + 2^{\frac{1}{2}}\epsilon^{-\frac{1}{2}}\Psi(\eta, -1) = 0, \tag{2.51}$$

$$Q(\eta, 1) = Q(\eta, -1) = 0. \tag{2.52}$$

Furthermore, equation (2.39) implies that Ψ is a function of η only which, for future convenience, we write as

$$\Psi = (\tfrac{1}{2}\epsilon)^{\frac{1}{2}} F'(\eta). \tag{2.53}$$

It then follows from equation (2.41) that

$$Q = H_x(\eta, x) + \{\nu\beta/2k(2g)^{\frac{1}{2}}\} F(\eta), \tag{2.54}$$

where $H_x(\eta, x)$ is a harmonic function which has yet to be determined. In view of (2.52)

$$H_x(\eta, 1) = H_x(\eta, -1) = -\{\nu\beta/2k(2\epsilon)^{\frac{1}{2}}\} F(\eta), \tag{2.55}$$

and H is odd in x.

We now use equation (2.40) to find that

$$V(\eta, x) = -(g/2\Omega^2 L) H_\eta - \{\nu\beta x/2k(2\epsilon)^{\frac{1}{2}}\} F'(\eta) - \tfrac{1}{2}\eta H_x + G(\eta). \tag{2.56}$$

$G(\eta)$ must be determined from the boundary conditions and, in particular, equations (2.50) and (2.51) imply that

$$V(\eta, 1) = -(g/2\Omega^2 L) H_\eta(\eta, 1) - \tfrac{1}{2}\eta H_x(\eta, 1) - \{\nu\beta x/2k(2\epsilon)^{\frac{1}{2}}\} F'(\eta) + G(\eta) = V_+(\eta) + 2^{\frac{1}{2}}\epsilon^{-\frac{1}{2}}\Psi(\eta, 1), \tag{2.57}$$

$$V(\eta, -1) = -(g/2\Omega^2 L) H_\eta(\eta, -1) - \tfrac{1}{2}\eta H_x(\eta, -1) + \{\nu\beta x/2k(2\epsilon)^{\frac{1}{2}}\} F'(\eta) + G(\eta) = -2^{\frac{1}{2}}\epsilon^{-\frac{1}{2}}\Psi(\eta, -1), \tag{2.58}$$

and, therefore, that

$$\frac{g}{\Omega^2 L}\left[H_\eta(\eta, 1) + \frac{\nu}{k}\frac{\beta\eta}{(2\epsilon)^{\frac{1}{2}}} F'(\eta)\right] + V_+(\eta) + 2F'(\eta) = 0. \tag{2.59}$$

We can proceed further only if we choose an explicit form for $V_+(\eta)$. We choose

$$V_+(\eta) = e^{i\kappa\eta}, \tag{2.60}$$

and we note that any characterization of the flow associated with equation (2.60) will apply generally to flows having lateral scale κ^{-1}.

With this choice of $V_+(\eta)$, the odd Harmonic function H is given by

$$H(\eta, x) = A\, e^{i\kappa\eta} \sinh \kappa x$$

and, according to equation (2.55),

$$F(\eta) = -(2k\sqrt{2\epsilon\kappa}\cosh\kappa/\nu\beta) A\, e^{i\kappa\eta}. \tag{2.61}$$

These,† together with equation (2.59) yield

$$-F'(\eta) = V_+(\eta)/\{2 + MR(\kappa)\}, \tag{2.62}$$

where

$$M = g\beta(\nu/\Omega)^{\frac{1}{2}}/k\Omega, \tag{2.63}$$

and

$$R(\kappa) = 1 - \sinh\kappa/\kappa\cosh\kappa. \tag{2.64}$$

Finally, equations (2.50) and (2.51) give

$$V(\eta, 1) = \frac{1 + MR}{2 + MR} V_+, \tag{2.65}$$

$$V(\eta, -1) = \frac{1}{2 + MR} V_+. \tag{2.66}$$

† H and F as given here are consistent with equations (2.57) and (2.58) because ηH_x is negligibly small under the previously imposed condition $a - 1 \ll 1$.

Figure (6) gives the curves of $(1+MR)/(2+MR) = \text{const.}$ in the (M, κ)-plane, but when M^{-1} and κ are both small, as is typical in geophysical situations,

$$V(\eta, 1) \simeq \frac{1+g\beta(\nu/\Omega)^{\frac{1}{2}}\kappa^2/3k\Omega}{2+g\beta(\nu/\Omega)^{\frac{1}{2}}\kappa^2/3k\Omega} V_+ = \frac{1+Z}{2+Z} V_+. \tag{2.67}$$

Clearly, if $Z \ll 1$, the motion resembles closely that of a fluid of uniform density. When $Z \gg 1$, the velocity varies continuously from V_+ at the top to zero at the bottom in conformity with the conjecture of the previous section. This paragraph can also be phrased as follows:

When the scale of the surface disturbance, the ambient density gradient and the transport properties are such that diffusion overwhelms convection in

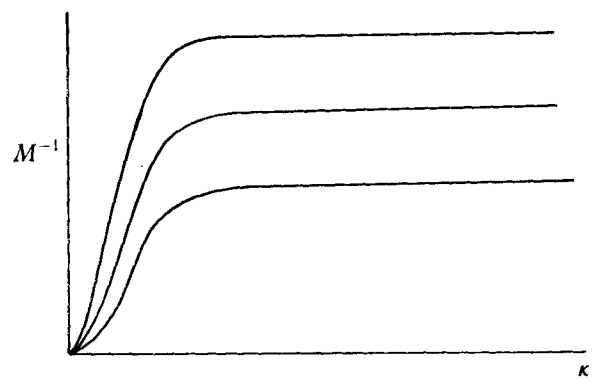

FIGURE 6. Curves of constant $(1+MR)/(2+MR)$.

maintaining the ambient density distribution, the fluid moves as though it were of uniform density. Alternatively, when the diffusive mechanisms are far too weak to compete with convection and maintain the ambient density field, the fluid moves in relatively isolated layers and the peripheral velocity varies smoothly from the value $V_+(\eta)$ at the top to zero at the bottom.

In geophysical situations, the diffusion mechanisms may be such that lateral diffusion is governed by a different diffusivity than is vertical diffusion. If one takes account of this anisotropy, the description of H preceding equation (2.61) would be modified to read

$$H(\eta, x) = e^{i\kappa\eta} \sinh \kappa' x,$$

where $\kappa' = \kappa(\nu_1/\nu_2)^{\frac{1}{2}}$ and ν_1, ν_2 are vertical and horizontal diffusion coefficients, respectively. This would affect both the *details* of the subsequent analysis and the precise definition of Z but, again, it would not affect the *character* of the flow.

3. Regions with bottom topography

In many geophysical situations, fluid moves in a region with an irregular bounding surface. In order to understand the implications of such irregular boundaries we seek the flows which occur in annular regions bounded at one end by the surface $x = b(\eta, \theta)$, and at the other by $x = 1$. Since the velocity and pressure fields will now depend on three independent variables we shall need to

extend the Ekman layer theory of the foregoing sections. The conservation equations are

$$u_\eta + v_\theta + w_x = 0, \tag{3.1}$$

$$-v + p_\eta = \epsilon \Delta u, \tag{3.2}$$

$$u + p_\eta = \epsilon \Delta v, \tag{3.3}$$

$$p_x = \epsilon \Delta w, \tag{3.4}$$

where u, v, w are the perturbation velocities referred to $R\Omega$, p is the dimensionless pressure perturbation, ϵ, η and x have already been defined and θ is the conventional angular co-ordinate multiplied by R/L. R is the mean radius of the annulus which is so narrow compared to R that, for example, the variable coefficient, $1/r$, in the tangential component of grad p has been replaced by $1/R$.

We again expect u, v, w, p to exhibit a boundary-layer structure and, since we are dealing with a fluid of uniform density again, we write

$$\begin{aligned}
u &= U(\eta,\theta) + u_1(\eta,\theta,\epsilon^{-\frac{1}{2}}\{x-1\}) + u_2(\eta,\theta,\epsilon^{-\frac{1}{2}}\{x-b\}),\\
v &= V(\eta,\theta) + v_1(\eta,\theta,\epsilon^{-\frac{1}{2}}\{x-1\}) + v_2(\eta,\theta,\epsilon^{-\frac{1}{2}}\{x-b\}),\\
w &= W(\eta,\theta) + w_1(\eta,\theta,\epsilon^{-\frac{1}{2}}\{x-1\}) + w_2(\eta,\theta,\epsilon^{-\frac{1}{2}}\{x-b\}),\\
p &= P(\eta,\theta) + p_1(\eta,\theta,\epsilon^{-\frac{1}{2}}\{x-1\}) + p_2(\eta,\theta,\epsilon^{-\frac{1}{2}}\{x-b\}).
\end{aligned}$$

In the boundary layers along $x = b(\eta,\theta)$ we have

$$p_{2,\theta} \simeq -b_\theta p_{2,x}, \quad p_{2,\eta} \simeq -b_\eta p_{2,x},$$

$\Delta w_2 \simeq \lambda^2 w_{xx}$, ..., and, using equations (3.4) and (3.1) to eliminate p_2 and w_2, equations (3.2) and (3.3) can be cast in the form

$$\epsilon(v_2 - iau_2)_{xx} = i\lambda^{-3}(v_2 - iau_2), \tag{3.5}$$

where $\lambda^2 = 1 + b_\theta^2 + b_\eta^2$ and $a = a_1 + ia_2 = (\lambda + ib_\eta b_\theta)/(1 + b_\theta^2)$.

It follows that

$$v_2 - iau_2 = [v_{20}(\eta,\theta) - iau_{20}(\eta,\theta)] \exp\{-(i/\epsilon\lambda^3)^{\frac{1}{2}}(x-b)\}, \tag{3.6}$$

where v_{20} and u_{20} have yet to be determined. Equation (3.1) can now be used to find w_2. We need only $w_2(\eta,\theta,0)$ which is given by

$$\begin{aligned}
w_2(\eta,\theta,0) = b_\eta u_{20} + b_\theta v_{20} &+ [(\tfrac{1}{2}\epsilon\lambda^3)^{\frac{1}{2}}\{v_{20} + (a_1 + a_2)u_{20}\}/a_1]_\eta\\
&+ [(\tfrac{1}{2}\epsilon\lambda^3)^{\frac{1}{2}}\{(a_1 - a_2)v_{20} - (a_1^2 + a_2^2)u_{20}\}/a_1]_\theta.
\end{aligned} \tag{3.7}$$

The terms of order $\epsilon^{\frac{1}{2}}$ must be retained if we are to analyse successfully the flow at and near points where $b_\eta = b_\theta = 0$.

The corresponding result is easily obtained for u_1, v_1, w_1. We need only $w_1(\eta,\theta,0)$ which is given by

$$w_1(\eta,\theta,0) = -(\tfrac{1}{2}\epsilon)^{\frac{1}{2}}[(v_{10} + u_{10})_\eta + (v_{10} - u_{10})_\theta]. \tag{3.8}$$

The boundary conditions require that

$$W(\eta,\theta) + w_2(\eta,\theta,0) = W(\eta,\theta) + w_1(\eta,\theta,0) = 0, \tag{3.9}$$

$$U(\eta,\theta) + u_2(\eta,\theta,0) = V(\eta,\theta) + v_2(\eta,\theta,0) = 0, \tag{3.10}$$

$$V(\eta,\theta) + v_1(\eta,\theta,0) = V_+(\eta,\theta), \tag{3.11}$$

$$U(\eta,\theta) + u_1(\eta,\theta,0) = U_+(\eta,\theta), \tag{3.12}$$

where V_+ and U_+ are prescribed in accord with the imposed surface motion at $x = 1$. If, away from the Ekman layers, the frictional terms are unimportant, then equations (3.2), (3.3) and (3.4) imply that

$$V = P_\eta \quad \text{and} \quad U = -P_\theta. \tag{3.13}$$

In fact, of course, lateral diffusion is locally important under particular circumstances and we must re-assess its role when the 'inviscid theory' associated with equation (3.13) has been completed.

Equations (3.7) through (3.13) can now be combined to give

$$(\tfrac{1}{2}\epsilon)^{\frac{1}{2}}[\{\lambda^{\frac{3}{2}}(P_\eta - a_2 P_\theta)/a_1\}_\eta + \{\lambda^{\frac{3}{2}}((a_1^2+a_2^2)P_\theta - a_2 P_\eta)/a_1\}_\theta + \Delta P] + b_\theta P_\eta - b_\eta P_\theta$$
$$= (\tfrac{1}{2}\epsilon)^{\frac{1}{2}}[(V_+ + U_+)_\eta + (V_+ - U_+)_\theta]. \tag{3.14}$$

Equation (3.14) can be manoeuvred into the form (neglecting terms in P_η and P_θ whose coefficients are of order $\sqrt{\epsilon}$)

$$(\tfrac{1}{2}\epsilon)^{\frac{1}{2}}[\Delta P + \lambda^{\frac{1}{2}}(\operatorname{grad} b)^2 P_{bb} + \lambda^{\frac{5}{2}}\{(\operatorname{grad} b)^2 + J^2\}P_{ss}] + JP_s$$
$$= (\tfrac{1}{2}\epsilon)^{\frac{1}{2}}[V_{+,\theta} + V_{+,\eta} + U_{+,\eta} - U_{+,\theta}]$$
$$= (\tfrac{1}{2}\epsilon)^{\frac{1}{2}} g(b,s), \tag{3.15}$$

where J is the Jacobian $J = b_\theta s_\eta - s_\theta b_\eta$, $\Delta = \partial^2/\partial\theta^2 + \partial^2/\partial\eta^2$, and s is a co-ordinate which measures distance along curves $b = \text{const.}$ Since P is a stream function for U and V, equation (3.14) must be solved subject to the boundary condition that P is constant on each cylindrical boundary of the annulus. If the tangential component of velocity fails to vanish on these surfaces, one must append another frictional boundary layer to rectify this local discrepancy.

In the next section we will display some details of the flow patterns for certain $b(\eta,\theta)$ but it is convenient, first, to explore the qualitative features of the flow for reasonably general $b(\eta,\theta)$. Suppose that $b(\eta,\theta)$ is such that some curves $b = \text{const.}$ are closed as are those labelled C in figure 7. On any single hill b and s can be defined explicitly and, in particular, for each value of b, there is an $s_0(b)$ such that the points $(b,0)$ and $(b, s_0(b))$ coincide. For the region over this hill then, we write

$$\mathscr{M}(P) = (\tfrac{1}{2}\epsilon)^{\frac{1}{2}}\mathscr{L}(P) + JP_s = (\tfrac{1}{2}\epsilon)^{\frac{1}{2}}[g(b,s) - G(b,s)] + (\tfrac{1}{2}\epsilon)^{\frac{1}{2}} G(b,s), \tag{3.16}$$

where $\mathscr{L}(P)$ is the second-order elliptic operator of (3.15),

$$G(b,s) = (1+\lambda^{\frac{1}{2}})(\operatorname{grad} b)^2 f(b),$$
$$f(b) = \int_0^{s_0(b)} (g/J)\,ds \Big/ \int_0^{s_0(b)} (A/J)\,ds,$$

and

$$A = (1+\lambda^{\frac{1}{2}})(\operatorname{grad} b)^2.$$

If $P^{(1)}$ and $P^{(2)}$ are defined as solutions of

$$P^{(1)}_{bb} = f(b) \tag{3.17}$$

and

$$JP^{(2)}_s = (\tfrac{1}{2}\epsilon)^{\frac{1}{2}}[g(b,s) - G(b,s)] \tag{3.18}$$

(a periodic solution, $P^{(2)}$, is assured by the definition of G), then $P^{(1)} + P^{(2)}$ is a solution of (3.16). There is a superficial difficulty near point D, at the top of the hill (where $A = 0$), but we note that, in the original co-ordinates, we have (near D)

$$(2\epsilon)^{\frac{1}{2}}\Delta P + JP_s = (\tfrac{1}{2}\epsilon)^{\frac{1}{2}} g. \tag{3.19}$$

If J is linear in the distance from D then there is a region whose size is of order $\epsilon^{\frac{1}{4}}$ in which the first derivatives of P are of order $\epsilon^{\frac{1}{4}}$ (so that each term of (3.19) is of order $\epsilon^{\frac{1}{2}}$) and which blends into the solution $P^{(1)}+P^{(2)}$. Other singular regions occur near 'stagnation points' such as F of figure 7. Again, depending on the local curvature of $b(\eta,\theta)$, one can expect velocities U, V, of order ϵ^{ν} with $0 \leqslant \nu \leqslant \frac{1}{2}$.

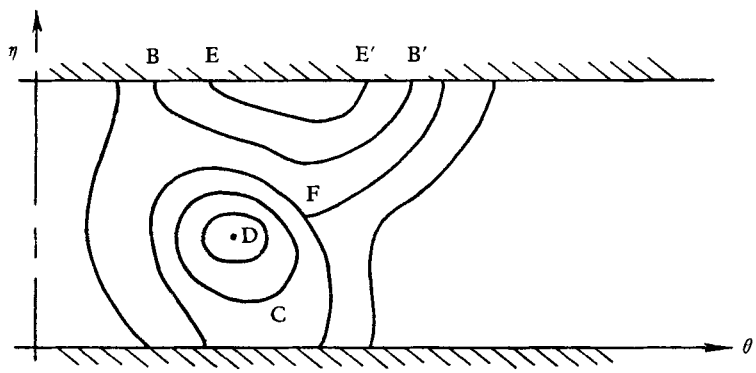

FIGURE 7. Curves b = const. relevant to the discussion following equation (3.15).

Thus, since the magnitude of $P_b^{(1)}$ is of order $|f|$, $P_\eta^{(1)}$ and $P_\theta^{(1)}$ must be of order $|V_{+,\eta}|/|\text{grad}\, b|$ and the flow *along* contour lines is at a speed of order $V_+ L_1/L_2$ where L_1 is the topographical scale and L_2 is the scale with which the imposed motion varies. Alternatively, the flow *across* contour lines is of order $\sqrt{\epsilon}\, L_1/L_2$. Intermediate speeds are to be expected in transition regions.

On stream lines such as BB′ or EE′ of figure 7 there is no requirement that $P^{(2)}$ be periodic in s. Accordingly, we cannot decompose the non-homogeneous term of equation (3.15) as we did in equation (3.16). In this case, the decomposition must be such that $P^{(1)}+P^{(2)}$ has the same value at each end of the streamline; that is, P_{wall} = const. Again, of course, the speed along contour lines is of order $V_+ L_1/L_2$ and that across contour lines is smaller by a factor $\sqrt{\epsilon}$.

Before turning to a specific topography and imposed surface motion we note that, if the surface tractions had been specified instead of the surface motion at $x = 1$, the term ΔP would be missing in equation (3.14) and the non-homogeneous term would be given in terms of surface tractions. Thus, the *character* of the phenomenon is not changed by this change in the driving specification.

3.1. *Some specific topographies*

Let
$$b(\eta,\theta) = (-1)^n C\left(\theta - \frac{n-1}{2N}\frac{2\pi R}{L}\right) \quad \text{in} \quad R_n, \tag{3.20}$$
where R_n is the region†
$$0 < \eta < 3\pi, \frac{n-1}{2N}\frac{2\pi R}{L} < \theta < \frac{n}{2N}\frac{2\pi R}{L},$$
and let
$$V_+(\eta,\theta) = \left\{\begin{array}{lll} 0 & \text{in} & 0 < \eta < \pi \\ \sin^2\eta & \text{in} & \pi < \eta < 2\pi \\ 0 & \text{in} & 2\pi < \eta < 3\pi \end{array}\right\} = h(\eta), \tag{3.21}$$

† Recall that the co-ordinate is so defined that $b(\eta,\theta) = b(\eta,\theta+2\pi R/L)$.

and $U_+(\eta,\theta) \equiv 0$ (see figures 8 and 9). For such a topography there are no closed contour lines and equation (3.14) has the form

$$(\tfrac{1}{2}\epsilon)^{\frac{1}{2}}[1+(1+C^2)^{\frac{1}{4}}](P_{\theta\theta}+P_{\eta\eta})+(-1)^n CP_\eta = (\tfrac{1}{2}\epsilon)^{\frac{1}{2}}h'(\eta) \quad \text{in} \quad R_n. \tag{3.22}$$

Clearly P is well approximated by $P^{(1)}$ where

$$P^{(1)} = (-1)^n(\tfrac{1}{2}\epsilon)^{\frac{1}{2}}h(\eta)/C, \tag{3.23}$$

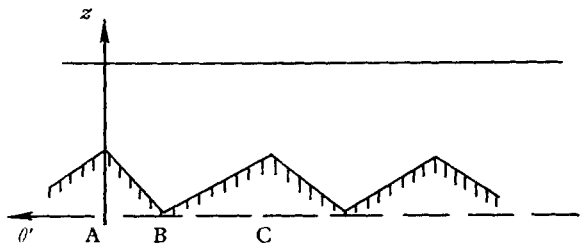

FIGURE 8. This geometry has period 2π in θ', the conventional angular co-ordinate. The co-ordinate θ in figure 10 is a constant multiple of θ'.

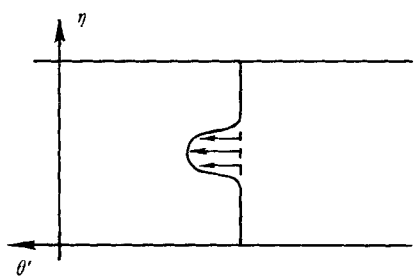

FIGURE 9. Circumferential surface velocity; η is the radial co-ordinate.

except in regions centring on $\theta = \pi nR/2NL$ and we describe the full solution in, say, $-\pi R/2NL < \theta < \pi R/2NL$ by

$$P = P^{(1)}+P^{(2)}(\eta,\theta/\epsilon^{\frac{1}{4}}). \tag{3.24}$$

$P^{(2)}$ must obey the equation

$$KP^{(2)}_{\xi\xi}(\eta,\xi)+(-1)^n P^{(2)}_\eta = 0, \tag{3.25}$$

where $K = [1+(1+C^2)^{\frac{1}{4}}]/\sqrt{2}C$ and $\xi = \theta/\epsilon^{\frac{1}{4}}$, and it must obey boundary conditions consistent with the fact that P and P_θ are continuous at $\theta = 0$. These boundary conditions are

$$\begin{aligned} P^{(2)}(0,\xi) &= P^{(2)}(3\pi,\xi) = 0, \\ P^{(2)}(\eta,0+) &= h(\eta)/C+q(\eta), \\ P^{(2)}(\eta,0-) &= -h(\eta)/C+q(\eta) \end{aligned}$$

and

$$P^{(2)}_\xi(\eta,0+) = P^{(2)}_\xi(\eta,0-) = f(\eta). \tag{3.26}$$

Here $q(\eta)$ is the as yet unknown function

$$q(\eta) = P(\eta,0),$$

and $f(\eta)$ is defined by equation (3.26).

It is clear that $P^{(2)}$ exists, although its details have yet to be explored. We need only note that the streamlines $P = \text{const.}$ must be as shown in figure 10, that the velocity is of order $\epsilon^{\frac{1}{4}}$ near $\theta = 0$, and that it is of order $\epsilon^{\frac{1}{2}}$ elsewhere.

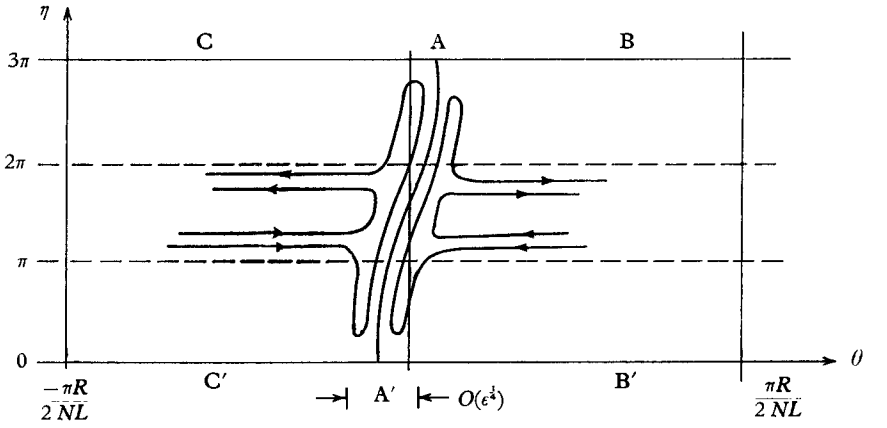

FIGURE 10. Flow over the topography of equation (3.20) with the surface motion of equation (3.21). The details near A and A′ are purely schematic; no detailed calculations have been made and frictional considerations (absent from this theory) would obliterate such details anyway. See also figures 8, 9 and 11.

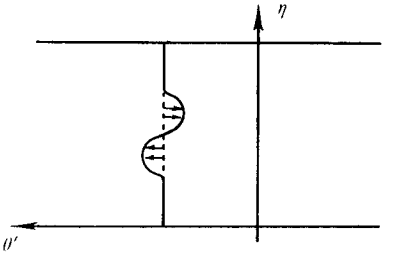

FIGURE 11. Circumferential velocity in regions like BB′ of figure 8. Over CC′ the velocity is the reverse of that shown here. The velocity scale is smaller than that of figure 9 by a factor $(\nu/\Omega L^2)^{\frac{1}{2}}$.

We now consider a topography for which $b(\eta, \theta)$ is that of equation (3.20) in $-\theta_0 = -\pi R/NL < \theta < \pi R/NL = \theta_0$ but for which $b(\eta, \theta) = 0$ in the rest of the region (see figure 12). Except in regions of width $\epsilon^{\frac{1}{4}}$ which lie in an $\epsilon^{\frac{1}{4}}$ neighbourhood of the ends (i.e. near $\theta = \pm\theta_0$), the flow in $-\theta_0 < \theta < \theta_0$ is the same as that of the previous problem, i.e. $P^{(1)}(\eta, \theta)$. However, in the rest of the domain $P = P^{(0)}(\eta, \theta)$ where

$$P^{(0)}_{\theta\theta} + P^{(0)}_{\eta\eta} = h'(\eta)$$

and $P(\theta, \eta)$,will describe the smooth surface which is conventionally visualized via the membrane analogy. The behaviour of $P(\eta, -\theta_0)$ and $P(\eta, \theta_0)$ can be determined only by appending to $P^{(1)}(\eta, \theta)$ boundary-layer contributions $P^{(3)}(\eta, \{\theta - \theta_1\}/\epsilon^{\frac{1}{4}})$ and $P^{(4)}(\eta, \{\theta - \theta_0\}/\epsilon^{\frac{1}{4}})$ for which, at θ_0,

$$P^{(0)}(\eta, \theta_0) = P^{(1)}(\eta, \theta_0) + P^{(4)}(\eta, 0),$$
$$P^{(0)}_{\theta}(\eta, \theta_0) = P^{(1)}_{\theta}(\eta, \theta_0) + P^{(4)}_{\theta}(\eta, 0).$$

Again the details are not important and the flow pattern is depicted in figure 13.

It is interesting to note that in the flat region of this problem

$$V = P_\eta^{(0)} \simeq h(\eta) - \frac{1}{3\pi}\int_0^{3\pi} h(\eta)\,dy$$
$$= h(\eta) - \tfrac{1}{6} \quad \text{in} \quad \theta_0 < \theta < 2\pi - \theta_0$$

(because there is no *net* peripheral flux of fluid) whereas, when $b \equiv 0$, V would be given by

$$V = h(\eta) \quad \text{for all } \theta.$$

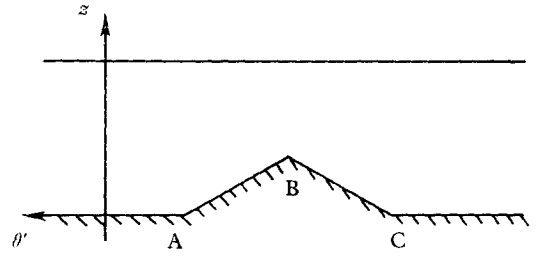

FIGURE 12. This geometry is also periodic in $0 < 0' < 2\pi$ but has only one bump.

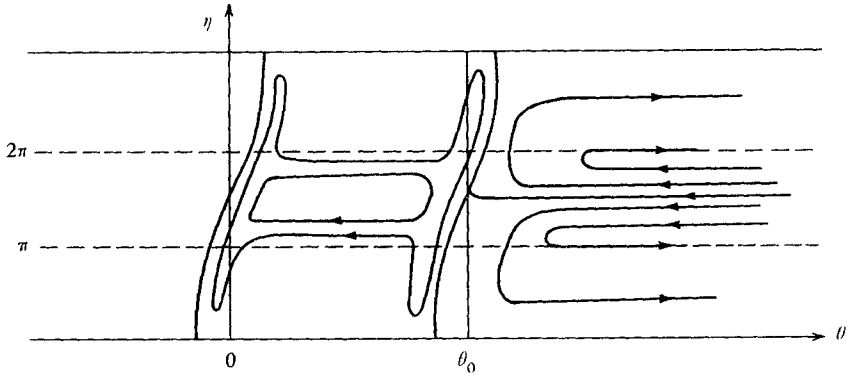

FIGURE 13. Flow pattern over

$$b(\eta, \theta) = \begin{cases} C\theta, & 0 < \theta < \theta_0 \\ -C\theta, & -\theta_0 < \theta < 0 \\ C\theta_0, & \text{elsewhere,} \end{cases}$$

with $V_+(\eta)$ as given by equation (3.21).

Thus, the 'hill' near $\theta = 0$, completely blocks (to order $\sqrt{\epsilon}$) the flow which would occur in the unimpeded container. The final flow is nearly described by the unimpeded flow plus a uniform flux-cancelling return flow.

The flow past an isolated hill or depression can be studied by adopting the particular geometry for which

$$b = 0 \quad \text{in} \quad 0 < \eta < \eta_1,$$

except in $\theta^2 + (\eta - \eta_2)^2 < R_1^2$, where (with $\eta_2 > R$ and $\eta_1 > \eta_2 + R_1$)

$$b(\eta, \theta) = C[R_1^2 - \theta^2 - (\eta - \eta_2)^2].$$

In the latter region, the natural co-ordinates are

$$\xi = [\theta^2 + (\eta - \eta_2)^2]^{\frac{1}{2}} \quad \text{and} \quad \alpha = \arctan[(\eta - \eta_2)/\theta].$$

In the region $\xi^2 < R_1^2$ we denote the pressure field by $P^{(5)}$; in the co-ordinates (ξ, α) equation (3.14) has the form

$$(\tfrac{1}{2}\epsilon)^{\frac{1}{2}}[1+(1+C^2)^{\frac{1}{4}}]P^{(5)}_{\xi\xi}+\xi P^{(5)}_{\alpha} = (\tfrac{1}{2}\epsilon)^{\frac{1}{2}}g(\xi,\alpha). \tag{3.27}$$

When $V_+(\eta)$ is linear in $\xi^2 < R_1^2$, $g(\xi,\alpha) = G = \text{const.}$, the solution of equation (3.27) is

$$P^{(5)} = G\xi^2/[1+(1+C^2)^{\frac{1}{4}}]+K, \tag{3.28}$$

and there is no flow across contour lines. We shall discuss the constant K later.

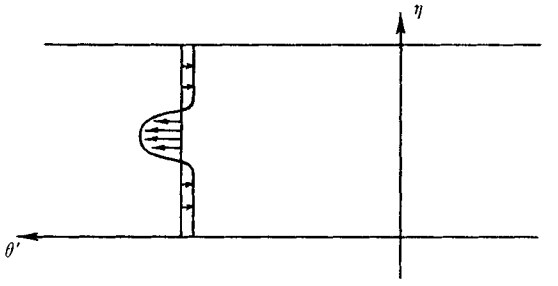

FIGURE 14. Circumferential velocity over flat part of figure 12. Net flux of fluid is zero.

We denote the pressure field outside of $\xi^2 = R_1^2$ by

$$P = P^{(6)}+P^{(7)}, \tag{3.29}$$

where $P^{(6)}_{\eta} = V_+(\eta)$ (this is the no-topography solution of § 2.1) and, in order that the pressure field of (3.29) match that of equation (3.28), $P^{(7)}$ is a harmonic function which must obey the boundary conditions

$$\begin{aligned} P^{(7)} &= 0 && \text{on} \quad \eta = 0, \\ P^{(7)} &= K_1 = \text{const.} && \text{on} \quad \eta = \eta_0, \\ P^{(7)}+P^{(6)} &= P^{(5)} && \text{on} \quad \xi = R_1, \end{aligned}$$

and is such that the top and bottom surfaces of the container exert no net force or net torque on the fluid. This last condition removes the lack of uniqueness ordinarily encountered in two-dimensional potential-flow problems. In fact, in the limit $R_1/\eta_1 \to 0$, these conditions are all met if $P^{(7)}$ vanishes on $\eta = 0$ and on $\eta = \eta_1$ and if, in equation (3.18), K has the value

$$K = -GR_1^2/[1+(1+C^2)^{\frac{1}{4}}].$$

Any other choice than $K_1 = 0$ implies that a non-vanishing net surface force in the θ-direction is applied to the fluid by the container surface; any other choice for K implies that the surface applies a torque about the point $\xi = 0$.

3.2. *The effects of lateral diffusion*

The flows described in § 3.1 each exhibit regions in which the velocity gradients have a scale of order $\epsilon^{\frac{1}{4}}$. We have already seen in [1] that lateral diffusion can play an important role in phenomena of this scale. We must conclude, then, that if any of the $\epsilon^{\frac{1}{4}}$ boundary layers associated with the foregoing analysis is thicker (by a

factor of 'a few') than the cylindrical diffusive layer which arose in [1], the effects of lateral diffusion will not be important and the descriptions of § 3.1 are valid.

This is the case when, for example, $C < \frac{1}{5}$ in the foregoing geometries. Conversely, if $C > 5$, the lateral boundary layers of the foregoing section are thinner than the diffusive layers of [1] and the details of the actual layers can only be obtained when frictional effects are taken into account. In the first two configurations of § 3.1, these frictional details cannot modify the flow field away from the layers but, in the third geometry, such a broad modification may occur. The results obtained by Jacobs (1964) strongly suggest that K and K_1 may be strongly influenced by the $\epsilon^{\frac{1}{4}}$ diffusive layer circumscribing the base of the hill. I say 'suggest' because his flow is driven in a very different manner from ours and I have not interpreted his result in the context of our flows.

3.3. *Two-layer flows with bottom topography*

We consider here the flow of two immiscible fluids whose interface is nearly horizontal and is well above the highest point on the lower boundary. The three-dimensional Ekman layer theory of § 3 can be used simply to show that, in the upper layer,

$$2\Delta P_1 = (V_+ + V_0 + U_+ + U_0)_\eta + (V_+ + V_0 - U_+ - U_0)_\theta \tag{3.30}$$

and that, in the lower layer,

$$\mathscr{L}(P_2) + 2^{\frac{1}{2}}\epsilon^{-\frac{1}{2}} J P_{2,s} = (V_0 + U_0)_\eta + (V_0 - U_0)_\theta, \tag{3.31}$$

where the operator $\mathscr{L}$ is defined after equation (3.16), V_+, U_+, are components of surface velocity, V_0, U_0, are components of interface velocity, and subscripts 1 and 2 refer to the upper and the lower fluid respectively. J and s have already been defined. The three-dimensional Ekman layer theory also implies (through the requirement for continuity of stress) that

$$(1+k)(V_0 + iU_0) = (V_1 + iU_1) + k(V_2 + iU_2), \tag{3.32}$$

where

$$k = (\mu_2\rho_2/\mu_1\rho_1)^{\frac{1}{2}}.$$

Equation (3.32) can be used to eliminate U_0, V_0 from equations (3.30) and (3.31), after which they can be manipulated into

$$\mathscr{L}(P_2) - [2k/(1+2k)]\,\Delta P_2 + (2/\epsilon)^{\frac{1}{2}} J P_{2,s} = [(V_+ + U_+)_\eta + (V_+ - U_+)_\theta]/(1+2k)$$
$$= g(\eta, \theta)/(1+2k) \tag{3.33}$$

and

$$\Delta P_1 = \frac{k}{1+2k}\Delta P_2 + \frac{1+k}{1+2k} g(\eta, \theta). \tag{3.34}$$

The former of these we have already discussed. It implies that (when $k \simeq 1$) P_2 is $1/(1+2k)$ of what it would be if there were a single fluid of uniform density present. For topography and surface motions like those of the first two problems of § 3.1, the velocity V_2, U_2, is always small (with $k \simeq 1$, it is $\frac{1}{3}$ that of those analyses). For the upper layer, then, it follows from the results of § 2.2 that

$$U_0 = U_1 \simeq 0 \tag{3.35}$$

and

$$V_1 = 2V_0 = \tfrac{2}{3}V_+(\eta). \tag{3.36}$$

For the third topography of § 3.1 the general problem is non-trivial and we shall not pursue its details here. However, when the topographical scale is small compared to that of $V_+(\eta)$, the discussion of § 3 again implies that $U_2^2 + V_2^2$ is small compared to $V_+^2(\eta)$ so that equations (3.35) and (3.36) are good approximations again.

To find P_1 and P_2 in the non-trivial case, we must solve equations (3.33) and (3.34) under boundary conditions which require that $P_1 = \text{const.}$, $P_2 = \text{const.}$ on each annular boundary. The lack of uniqueness inherent in this incomplete statement must be removed by the requirement that the net force or torque applied to either fluid via the surface tractions is zero. Note that, even in the simple situation where $b \equiv 0$, equation (3.15) leads to the results of [1] and of § 2.1, only when this 'no net traction' requirement is applied. This difficulty arises in the three-dimensional formalism because the surface motions appear in the equations only as $V_{+,\eta}$, $V_{+,\theta}$, etc.

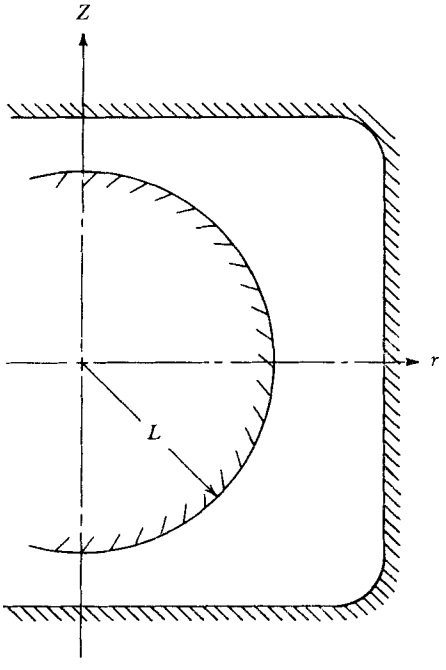

FIGURE 15. Characterizing geometry of § 7.

4. Flows in equatorial regions

We study here the flow in regions whose geometry is typified by that of figure 15. The inner boundary is spherical, but the other boundary may be such that the flow is not axially symmetric. To deal with such flows, a formalism which differs markedly from those in the preceding sections is needed. This need is occasioned by the fact that the diffusive layer near the equator in which, for example, $|\partial v/\partial r| \gg |\partial v/\partial z|$ and $|u| \ll |w|$ must blend into those at larger z where $|\partial v/\partial r| \ll |\partial v/\partial z|$ and $|w| \ll |u|$. Accordingly, we must first develop a boundary-layer theory for the equatorial region.

The dimensionless conservation equations (again) are

$$v + p_\eta = \epsilon \Delta u, \tag{4.1}$$

$$-u + p_\theta = \epsilon \Delta v, \tag{4.2}$$

$$p_x = \epsilon \Delta w, \tag{4.3}$$

$$u_\eta + v_\theta + w_x = 0. \tag{4.4}$$

The notation is that of § 3 except that L is the radius of the sphere (see figure 15).

We take advantage of the fact that $|u| \ll |v|$ and that the characteristic length in the η (radial) direction is smaller than that in other directions and anticipate that the final term of equation (4.1) can be omitted. This omission can be justified when the theory has been developed by making the usual order-of-magnitude comparisons.

With equation (4.1) replaced by

$$v = -p_\eta, \tag{4.5}$$

it is convenient to write

$$w = -\psi_\eta, \tag{4.6}$$

and to note that equation (4.4) implies that

$$u = p_\theta + \psi_x + g(\theta, x), \tag{4.7}$$

where the constraints which determine $g(\theta, x)$ will arise in the context of each particular problem.

When equations (4.5) to (4.7) are substituted into equations (4.2) and (4.3), we obtain

$$\epsilon \Delta \psi_\eta + p_x = 0,$$

$$\epsilon \Delta p_\eta - \psi_x = g(\theta, x),$$

and since $|\psi_\eta| \gg |\psi_x|$ or $|\psi_\theta|$ and since $|v_\eta| \gg |v_x|$ or $|v_\theta|$, these can be approximated by

$$\epsilon \psi_{\eta\eta\eta} + p_x = 0,$$

$$\epsilon p_{\eta\eta\eta} - \psi_x = g(\theta, x).$$

Thus, with $\psi - ip = \chi$, we have

$$\epsilon \chi_{\eta\eta\eta} + i\chi_x = -ig(\theta, x). \tag{4.8}$$

It is now convenient to adopt a new co-ordinate system in which one co-ordinate measures distance from the equator along the spherical boundary, another measures distance from the spherical boundary and θ is unchanged. We choose

$$\xi = \epsilon^{-\frac{1}{3}} x \quad \text{and} \quad t = \epsilon^{-\frac{2}{3}}(\eta + \tfrac{1}{2}x^2), \tag{4.9}$$

and equation (4.8) becomes

$$\chi_{ttt} + i(\chi_\xi + \xi \chi_t) = -iG(\theta, \xi). \tag{4.10}$$

At this stage one could verify that, in a singular perturbation scheme whose largest contribution is described in these co-ordinates, the terms omitted in the foregoing do, indeed, belong in higher-order parts of the theory. One could also

verify that for axially symmetric flows, u is given by ψ_x and that, in equation (4.10), $G(\theta, \xi) \equiv 0$. This statement can be extended to say: when $p_\theta = \text{const.} \neq 0$ and $\mathbf{v}$ is independent of θ, u is again given by ψ_x (without loss of generality) and $G = -p_\theta$.

In the study of any specific phenomenon, one must find $\chi(t, \theta, \xi)$ and $G(\theta, \xi)$ in conformity with (4.10) and the boundary conditions appropriate to the equatorial region. Furthermore, χ must match the description of the flow which applies to the non-equatorial regions.

4.1. *Flow in a thin spherical annulus*

We seek here the flow which occurs when the angular velocity $\hat{\mathbf{z}}\Omega$ of one of the spherical shells of figure 16 differs slightly from the velocity $\hat{\mathbf{z}}\Omega'$ of the other. We adopt the average of these to describe the reference state and we measure t

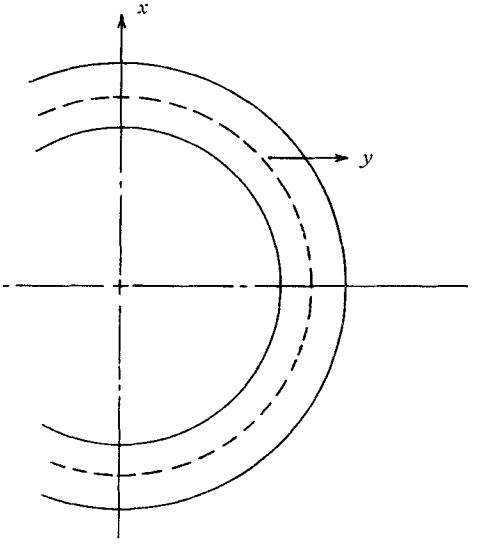

FIGURE 16. Configuration of § 7.1. y measures distance from the broken surface as shown.

from the spherical surface which bisects the region. We confine ourselves, in this section, to situations in which t_1 (see figure 16) is of order unity or less and we seek the flow in the equatorial region. We shall establish in a very simple way that this flow will match the flow for larger $|x|$ whose description is implied by § 2.1.

It is convenient once more to modify the co-ordinate system. We define

$$y = t/t_1, \quad \alpha = \xi t_1^2, \quad \beta = t_1^5,$$

and equation (4.1) becomes† (recalling that $G \equiv 0$ for axially symmetric flows)

$$\chi_{yyy} + i\alpha\chi_y = -i\beta\chi_\alpha. \tag{4.11}$$

† In view of the multiplicity of co-ordinate transformations, it may be useful to remind the reader that α is an appropriately scaled axial co-ordinate which vanishes in the equatorial plane and y is a (cylindrically) radial co-ordinate measured from a conveniently chosen spherical surface. In this problem the flow-region is $-1 < y < 1$.

Since χ should be analytic in β, we can describe $\chi(y,\alpha,\beta)$ by

$$\chi(y,\alpha,\beta) = \chi^{(0)}(y,\alpha) + \beta\chi^{(1)}(y,\alpha) + \ldots \tag{4.12}$$

and, when β is small enough, this description should be useful. We adopt as boundary conditions

$$\chi_y(\pm 1,\alpha,\beta) = \mp i, \tag{4.13}$$

$$\mathrm{Re}\,[\chi(\pm 1,\alpha,\beta)] = 0, \tag{4.14}$$

and we obtain for $\chi^{(0)}$

$$\chi^{(0)} = -i(\cosh ys - \cosh s)/s\sinh s + if(\alpha), \tag{4.15}$$

where $s = (i\alpha)^{\frac{1}{2}}$, $\arg s = -\frac{1}{2}\pi$ when $\alpha > 0$, $\arg s = \frac{1}{4}\pi$ when $\alpha < 0$, and, until further constraints arise, $f(\alpha)$ is any real function of α.

The function $\chi^{(1)}$ is that solution of

$$\chi^{(1)}_{yyy} - s^2\chi^{(1)}_y = -i\beta\chi^{(0)}_\alpha, \tag{4.16}$$

which is consistent with equations (4.13) and (4.14). It is given by

$$\begin{aligned} i8s^5\sinh^2 s\chi^{(1)} = {} & (5\sinh s + 2s\cosh s)\, y\cosh sy - sy^2\sinh s\sinh sy + 4sy \\ & + 4y\sinh s\cosh s - 8iyf's^3\sinh^2 s - k(s)\sinh sy. \end{aligned} \tag{4.17}$$

The last term is a solution of the homogeneous equation and equation (4.17) satisfies the boundary conditions only if

$$\begin{aligned} f' &= \mathrm{Im}\left[\frac{s^2+9}{s^2} - \frac{1}{s\sinh s\cosh s} - \frac{4\cosh s}{s\sinh s} - \frac{6}{\sinh^2 s}\right] \Big/ 8\,\mathrm{Re}\,[s\tanh s] \\ &= \mathrm{Im}\,[A]/8\,\mathrm{Re}\,[s\tanh s], \end{aligned} \tag{4.18}$$

$$k = s\sinh s\, g(\alpha) + 9\cosh s + 6s/\sinh s$$

and

$$g(\alpha) = \frac{\mathrm{Im}\,[sA/\sinh s]}{\mathrm{Im}\,[s\coth s]}. \tag{4.19}$$

One could go on with this but it seems informative to record only the following:

$$\begin{aligned} \chi_y(y,0,\beta) = -i[& +y + \beta(1-y^2)(11-4y^2+y^4)/720 \\ & + \beta^2 y(1-y^2)(4869 - 767y^2 + 53y^4)/(720\times 5040) + \ldots], \end{aligned} \tag{4.20}$$

and

$$\chi_y(y,\alpha,\beta) \sim -i\begin{Bmatrix} e^{s(y-1)} & \text{near} & y = +1 \\ e^{-s(y+1)} & \text{near} & y = -1, \end{Bmatrix} \tag{4.21}$$

for $\alpha \gg 1$.

Equation (4.20) indicates clearly that when $\beta \ll 60$, the flow at the equator is entirely controlled by local friction but that, as we consider regions with larger β (recall that $\beta = t_1^5$) the velocity profile becomes distorted and it is clear that the Ekman layers at large α are exchanging fluid with the equatorial region. The large α description of equation (4.21) is precisely the result which would have been obtained by the analysis of § 2.1. Hence, that analysis and the foregoing result describe the whole flow field for $\beta \leqslant 30$ (i.e. for $t_1 \leqslant 2$, an annulus whose spacing is not more than $4R(\nu/\Omega R^2)^{\frac{2}{5}}$). Further details can be extracted, of course, but in the absence of a specific context, such details are not very interesting. Figure 17 depicts the velocity $v(y,0,2)$.

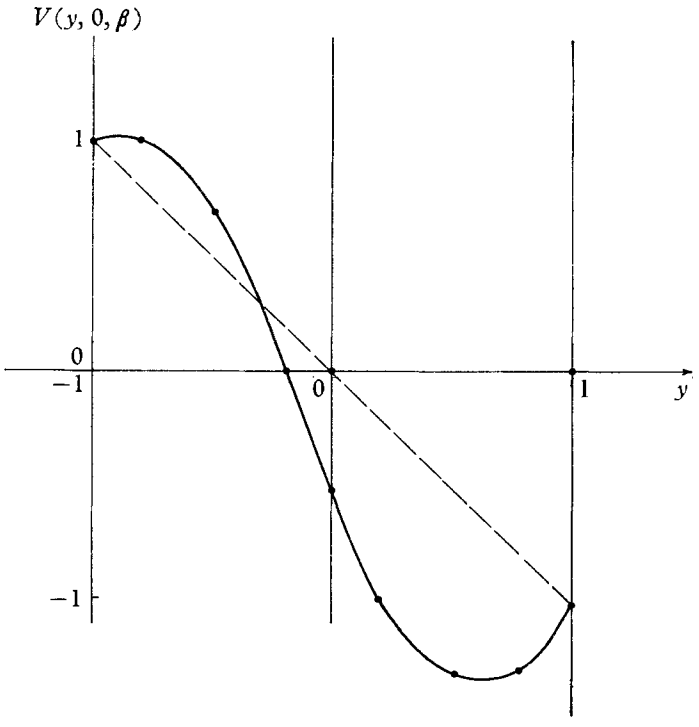

FIGURE 17. $V(y, 0, 2)$ for flow in figure 16 as given by equation (4.20).

4.2. *Other thin-layer flows*

In this section we ask whether there are flows in a thin region, $-h(\alpha) < y < 0$, $\theta_0 < \theta < \theta_1$, for which the velocity field is independent of θ and for which $p_\theta = \text{const.} \neq 0$. At the top of the layer, the dimensionless surface tractions $v_y = -1$, $\psi_{yy} = 0$ are given and, on $y = -h(\alpha)$, we require in problem (a) that $v_y = \psi_{yy} = 0$ (tangential stresses vanish) and, alternatively, in problem (b) that the velocity vanish. In each problem no fluid crosses $y = 0$ or $y = -h(\alpha)$. We shall find that, in each case there is a family of geometries for which such flows are possible and that one flow differs macroscopically from another in the net amount of fluid that is transported in the θ-direction.

To treat these problems conveniently we again need a mild modification of the co-ordinate system. We define $\zeta = y/h(\alpha)$ so that equation (4.10) becomes

$$\chi_{\zeta\zeta\zeta} - s^2h^2\chi_\zeta = ih^3D - i\beta h^3\chi_\alpha + i\beta h'h^2\zeta\chi_\zeta, \tag{4.22}$$

where D is the constant $-p_\theta$. We again describe the solution as a power series in β, i.e.

$$\chi = \chi^{(0)} + \beta\chi^{(1)} + \ldots, \quad h = h^{(0)}(\alpha) + \beta h^{(1)}(\alpha) + \ldots.$$

We obtain as an equation for $\chi^{(0)}$

$$\chi^{(0)}_{\zeta\zeta\zeta} - s^2h_0^2\chi_\zeta = -ih_0^3D. \tag{4.23}$$

For problem (a), the boundary conditions are

$$\chi^{(0)}_{\zeta\zeta}(-1, \alpha) = \operatorname{Re}\chi^{(0)}(-1, \alpha) = \operatorname{Re}\chi^{(0)}(0, \alpha) = 0$$

and

$$\chi^{(0)}_{\zeta\zeta}(0, \alpha) = -i/h_0^2,$$

and we obtain the solution

$$\chi^{(0)} = i(\zeta+1)/s^2 - i\sinh s(\zeta+1)/s^2\sinh s + iE_1(\alpha), \tag{4.24}$$

where $D = 1$, $h_0(\alpha) \equiv 1$, and, unless further constraints arise, the equation governing $\chi^{(1)}$ is

$$\chi^{(1)}_{\zeta\zeta\zeta} - s^2\chi^{(1)}_{\zeta} = 2s^2h_1\chi^{(0)}_{\zeta} - i\chi^{(0)}_{\alpha} - 3ih_1.$$

We obtain

$$\chi^{(1)} = \frac{i(\zeta+1)^2\cosh[s(\zeta+1)]}{8s^5\sinh s} - \frac{7i(\zeta+1)\sinh[s(\zeta+1)]}{8s^6\sinh s}$$
$$- \frac{i(\zeta+1)\cosh s\sinh[s(\eta+1)]}{4s^5\sinh^2 s} - \frac{ih_1(\eta+1)\cosh[s(\zeta+1)]}{s^4\sinh s} + \frac{ih_1(\zeta+1)}{s^2}$$
$$- \frac{E_1'(\alpha)(\zeta+1)}{s^2} + A\sinh[s(\zeta+1)] + B\{\cosh[s(\zeta+1)] - 1\} + iE_2(\alpha), \tag{4.25}$$

and

$$\chi^{(1)}_{\zeta\xi} = \frac{i(\zeta+1)^2\cosh[s(\zeta+1)]}{8s^3\sinh s} - \frac{3i(\zeta+1)\sinh[s(\zeta+1)]}{8s^4\sinh s}$$
$$- \frac{3i\cosh s(\eta+1)}{2s^5\sinh s} - \frac{i\cosh s\{2\cosh[s(\zeta+1)] + s(\zeta+1)\sinh[s(\zeta+1)]\}}{4s^4\sinh^2 s}$$
$$- i/s^6 - \frac{2ih_1 s}{2s\sinh s}\{s(\zeta+1)\cosh[s(\zeta+1)] + \sinh[s(\zeta+1)]\}$$
$$+ A^{(1)}s^2\sinh[s(\zeta+1)] + B^{(1)}s^2\cosh[s(\zeta+1)], \tag{4.26}$$

where $E_2(\alpha)$ is again a real function to be chosen later and A and B are the as yet unknown coefficients of the solutions of the homogeneous equations. Equations (4.25) and (4.26) are included only to support the following comments: the constant B is determined explicitly from equation (4.26) when we require that $\chi^{(1)}_{\zeta\zeta}(-1,\alpha) = 0$. The constant A is determined from (4.26) in terms of the unknown real number h_1 by requiring that $\psi^{(1)}_{\zeta\zeta}(0,\alpha) = 0$. The number h_1 is obtained from (4.25) by requiring that $\mathrm{Re}\,\chi(0,\alpha) = 0$. Note, in particular, that no constraints appear which help determine $E_1(\alpha)$ or $E_2(\alpha)$. These functions disappear from each substitution into a boundary condition. Furthermore, when one continues the process to find $\chi^{(2)}$, $E_1(\alpha)$ does appear in the determination of $A^{(2)}$ (the counterpart of $A^{(1)}$) from the counterpart of equation (4.26). In fact, $A^{(2)}$ is determined in terms of h_2 and $[E'(\alpha)/\alpha]'$. The requirement that $\mathrm{Re}\,\chi^{(2)}(0,\alpha) = 0$ then leaves open the choice of $[E_1'(\alpha)/\alpha]'$. As the process is continued the same freedom of choice arises for $E_2(\alpha), \ldots$. With each such choice of $E_n(\alpha)$, $h_n(\alpha)$ is implied (by $\mathrm{Re}\,\chi^{(n)}(0,\alpha) = 0$). Thus, there is a family of bottom contours $h(\alpha)$ to which there corresponds a family of flow fields for which p_θ is constant and among which the values of $\int_{-1}^{0} V\,d\zeta$ vary significantly. We note, in particular, that $h_1 = 1/720$ and that various choices for $E_1(0) \ll (1)$ leads to the velocity profiles of figure 18 when terms of order β are included and when $\beta = O(30)$.

The geophysical implications of this study will be indicated in the next section. We note there, however, that the variety of flows which can be constructed in this way is limited only in that the choice of $E_n(\alpha)$ must not imply such large

slopes $h_n'(\alpha)$ that equation (4.22) is inapplicable and they must not imply such large contributions to the higher-order terms that the series cannot be interpreted readily.

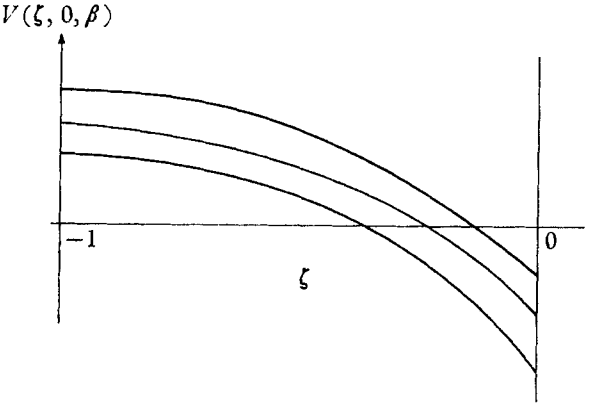

FIGURE 18. $V(\zeta, 0, \beta)$ for configuration of § 4.2, problem (*a*) for various $h(\alpha)$ (schematic only).

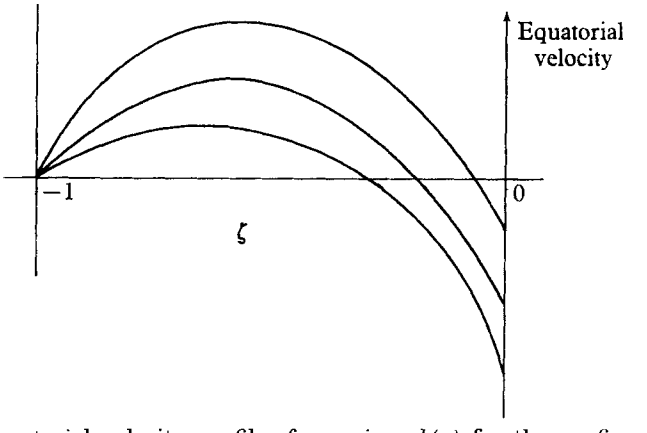

FIGURE 19. Equatorial velocity profiles for various $h(\alpha)$ for the configuration of § 4.2, problem (*b*). Note that, in general, both here and in figure 18, the net mass flux $\int_{-1}^{0} V\,d\zeta$ differs from zero and the 'turn around' mechanisms at $\theta = 0, \theta = \theta_0$, will determine which flow fits a given, fully prescribed situation.

When, under (*b*), we require that the velocity vector vanish on $\zeta + 1 = 0$, we obtain,

$$\chi^{(0)} = \frac{i(1+h_0\zeta)}{s^2} - \frac{i\cosh[sh_0(\zeta+1)]}{\cosh sh_0} - \frac{i\sinh sh_0\eta}{s^3\cosh sh_0} + iE_1(\eta),$$

where $h_0(\alpha)$ is implied by

$$\mathrm{Re}\left[\frac{-1}{s^2\cosh sh_0} + \frac{i(1-h_0)}{s^2} + \frac{i\tanh sh_0}{s^3}\right] = 0,$$

which implies that

$$h_0(0) = 25/16 \quad \text{and} \quad h_0(\alpha) \sim 1 + (2\alpha)^{-\frac{1}{2}} \quad \text{for} \quad \alpha \gg 1.$$

With an unreasonable amount of algebraic manipulation, the reader could verify that various choices of $h_1(0)$ lead to the velocity profiles of figure 19. Again we

see that the θ-independent flow for various bottom contours $h(\alpha)$ may differ greatly in the net transport of fluid in the θ-direction.

5. Geophysical considerations

Much of the ocean consists of two layers of fluid with relatively uniform density separated by the thermocline, a layer of relatively large density gradient. The bottom topography is extremely irregular. It is clear from the results of § 3 that the motion in the lower layer should differ greatly from that in the upper layer and it is well known that this is the case. However, it is not quite as easy to identify the 'correct' model for the upper layer. If the parameter Z of equation (2.67) is small compared to unity, as I estimate it to be, the upper layer acts largely as though it were of constant density and the results of § 3.3 are appropriate. Such a model leads to the prediction of motions which differ from those of a model in which (*a*) the interface is slippery, or (*b*) the interface is motionless, by factors of the order $\frac{3}{2}$. The work of § 3.3 should also permit the study of large-scale lower layer motions which are driven by the surface tractions at the ocean-atmosphere interface. Strong limitations on the utility of this model (or any other simple model) are implicit in the irregularity of the density structure of the ocean, the turbulent character of the transport processes and the fact that many intense currents in the upper layer may require a non-linear theory.

The Cromwell current, a surprisingly uniform equatorial undercurrent which is found in the Atlantic and the Pacific (Knauss 1960), can be discussed in relation to the work of § 4.2. The flows studied in that section are driven in the same way that the Cromwell current is driven. However, there is no reason to believe that the interface (thermocline) lies precisely at either the surface of zero tangential stress or the surface of vanishing velocity. Nevertheless, the fact that the analysis of § 4.2 displays velocity profiles which resemble that of the Cromwell current and which blend smoothly into acceptable higher-latitude flows suggests strongly that the dynamics of the Cromwell current can be understood within the framework of the theory of § 4. The simplest acceptable analysis would seem to require a two-layer model; in the upper layer a small-β ($\beta < 60$) theory would be appropriate but the lower layer is comparatively thick and is driven by the upper layer at all high latitudes. A two-layer study of the equatorial flow field would be very valuable.

In brief then, the foregoing material should provide a framework within which many facets of ocean-current dynamics can be studied and the adequacy of various 'models' can be tested.

The author greatly appreciates the hospitality of the University of Western Australia, where this work was performed, and the support of the Guggenheim Foundation and a Fulbright Grant whose generosity made this visit possible.

REFERENCES

Carrier, G. F. 1965 Phenomena in rotating fluids. To be published in the *Proc. 11th Int. Congr. Appl. Mech.*

Jacobs, S. 1964 The Taylor column problem. *J. Fluid Mech.* **20**, 581.

Knauss, J. 1960 Measurements of the Cromwell current. *Deep Sea Res.* **6**, 256–86.